Thermal Degradation and Ageing Behavior of Microcomposites of Natural Rubber, Carboxylated Styrene Butadiene Rubber Latices, and Their Blends

Ranimol Stephen,[1] A. M. Siddique,[2] Fouran Singh,[2] Lekshmi Kailas,[3] Seno Jose,[1] Kuruvilla Joseph,[4] Sabu Thomas[1]

[1]*School of Chemical Sciences, Mahatma Gandhi University, Kottayam 686 560, Kerala, India*
[2]*Materials Science Division, Inter University Accelerator Centre, Aruna Asaf Ali Marg, New Delhi, India*
[3]*Department of Physics and Astronomy, University of Sheffield, Sheffield, South Yorkshire S3 7RH, United Kingdom*
[4]*Department of Chemistry, St. Berchmans' College, Changanasserry, Kottayam, Kerala, India*

Received 20 October 2006; accepted 10 December 2006
DOI 10.1002/app.26042
Published online 13 March 2007 in Wiley InterScience (www.interscience.wiley.com).

ABSTRACT: The effect of microfillers on the thermal stability of natural rubber (NR), carboxylated styrene butadiene rubber (XSBR) latices, and their 70/30 NR/XSBR blend were studied using thermogravimetric method. Microcomposites of XSBR and their blend were found to be thermally more stable than unfilled samples. The activation energy needed for the degradation of polymer chain was calculated from Coats-Redfern plot. Activation energy needed for the thermal degradation of filled samples was higher than unfilled system. It indicated the improved thermal stability of the filled samples. The ageing resistance of the micro-filled samples was evaluated from the mechanical properties of aged samples. The thermal ageing was carried out by keeping the samples in hot air oven for 7 days at 70°C. The mechanical properties such as tensile strength, modulus at 300% elongation, and strain at break were computed. As compared to unfilled samples, micron-sized fillers reinforced systems exhibited higher ageing resistance. Finally, an investigation was made on the influence of ion-beam irradiation on microcomposites of NR, XSBR latices, and their 70/30 blend systems using $^{28}Si^{8+}$ performed at 100 MeV. The surface changes of the samples after irradiation were analyzed using X-ray photoelectron spectroscopy. The results of XPS measurements revealed that the host elements were redistributed without any change in binding energies of C_{1s}, O_{1s}, and Si_{2p}. © 2007 Wiley Periodicals, Inc. J Appl Polym Sci 105: 341–351, 2007

Key words: natural rubber; carboxylated styrene butadiene rubber; latex blends; micro fillers; thermal degradation; ageing; ion-beam irradiation

INTRODUCTION

Thermogravimetric analysis (TGA) of a polymeric material gives information about the stability and thermal degradation. A detailed understanding of the degradation characteristics of polymers on heating is essential for selecting materials with improved properties for specific application. It measures the change in weight of the material when it is heated against temperature in an inert atmosphere or in the presence of air or oxygen. When a compounded rubber is heated, the polymer part will get degraded first and converted into gaseous products. Further heating will remove all organic matter, giving the weight of inorganic components in the compound. The thermal degradation of polymers followed two paths, viz, unzipping and random. The unzipping mechanism gives the pure monomer while the random degradation leads to the formation of host products, depending on the structure of the polymer. Most of the polymers have a carbon–carbon (C—C) chain as the backbone; hence, their thermal stability depends on the stability of the C—C bond. The degradation of polymers is affected by the substituents in the backbone chain. The higher number of substituents usually decreases its thermal stability while the aromatic groups in a polymer backbone increase the thermal stability. The presence of oxygen atom and branching makes the polymer more susceptible to degradation. Thermal stability means the ability of a material to maintain the required properties such as strength, toughness, or elasticity at a given temperature. The assessment of thermal stability of polymeric materials can provide valuable technical information.[1] The demand for polymers, which could be used in high temperature applications, stimulated the investigations to unravel the relationship between thermal properties and chemical structure.[2] The addition of particulate fillers to elastomers resulting in enhancement in stiffness and resistance to fracture is one of the most important phenomena in material

Correspondence to: S. Thomas (sabut@sancharnet.in) or (sabut552001@yahoo.com).

science and technology. The commonly used white fillers in rubber industry are clay and silica. Because of the presence of hydroxyl groups on silica it shows higher filler–filler interactions resulting in poor dispersion in rubber when compared to other fillers.[3–4] Polymers having polar substituents exhibit better polymer–filler interaction on adding silica. Venter et al.[5] studied the thermal stability of silica filled SBR/BR composite. In the presence of silica particles, the decomposition temperature is shifted to higher temperature, which indicates better polymer/filler interaction. The high surface polarity of silica due to silanol groups leads to the agglomeration of filler particles. It has been shown that thermal ageing resistance of silica filled chlorinated poly (ethylene) (CPE)/natural rubber (NR) blends does not change significantly with an increase in silica loading.[6]

Synthetic latices do not exhibit the variability of natural latices due to the control, which is exercised over their preparation. Therefore, the blending of two latices is technically relevant for the end product applications. Because of strain induced crystallization behavior of NR, it possesses higher tensile strength and viscosity than synthetic latices. However, NR latex films exhibit poor modulus, stability towards fillers, thermal resistance, and gas barrier properties. Carboxylated styrene butadiene rubber (XSBR) latex offers excellent thermal stability, gas barrier properties, and good modulus, but it shows poor film formation ability and tensile strength. Thomas and coworkers[7–8] studied the mechanical, viscoelastic, and gas barrier properties of NR/XSBR latex blends. Venter et al.[5] studied the thermal stability of silica filled SBR/BR composite. In the presence of silica particles, the decomposition temperature is shifted to higher temperature, indicating improved polymer/filler interaction. The thermal ageing resistance of silica filled CPE/NR blends does not change significantly with an increase in silica loading.[6]

This paper deals with the thermal stability and ageing properties of microcomposites of NR, XSBR, and 70/30 NR/XSBR systems. Thermal ageing of polymers occurs as a result of chain scission, crosslink formation, and crosslink breakage. Thomas and coworkers[9–12] studied the ageing behavior of polymer blends and composites. Thermal degradation of particulate filled latices have analyzed by thermogravimetric method. A detailed understanding about the thermal stability of polymers is essential for determining the service life and the field of application. Varkey et al.[13] investigated the thermal degradation of NR/SBR latex blends by thermogravimetric method. They found that blending with SBR increases the thermal stability of NR. The stability of rubber vulcanizates depends on environment because degradation is primarily dependent on thermal or thermooxidative degradation. Li et al.[14] analyzed the thermal decomposition of chlorinated NR from latex at different atmospheres.

Many researchers have shown much interest on the studies of the chemical and physical structural modifications in the polymeric material induced by ion-bombardment. There are a lot of investigations have been performed to characterize the induced changes in polymers originated from ion-matter interactions, including changes in the resistance to solvents, in the optical and in electrical properties.[15–22] The macroscopic properties can be changed irreversibly by ion bombardment of polymeric materials. Electronic excitation, ionization, chain scission, and crosslinks as well as mass losses are the fundamental events observed in polymers due to ion beam irradiation.[23–25] These processes will depend on the target characteristics and implantation conditions, which include ion mass, energy, fluence, current density, and target temperature.[26]

EXPERIMENTAL

Materials used

Centrifuged NR with 60% dry rubber content used was collected from Gaico Rubbers, Kuravilangadu, Kerala, India. The synthetic latex XSBR having 47% dry rubber content was procured from Apar Industries, Mumbai, India. The characteristics of latices used are presented in Table I. Composition of particulate fillers such as clay and silica are shown in Table II.

Thermogravimetric analysis

Mettler Toledo Star SW7 was used for the thermogravimetric analysis (TGA). Samples were scanned from 30 to 600°C at a heating rate of 20°C/min.

Ageing studies

Thermal ageing

Ageing of filled samples was carried out by keeping the samples in hot air oven at 70°C for 7 days. Mechanical properties such as tensile strength, elongation at break, and secant modulus of the aged samples were analyzed as a function of filler loading.

Ion-beam irradiation

The latex films of 1 × 1 cm^2 dimension were irradiated with $^{28}Si^{8+}$ ion beam of 100 MeV in the General Purpose Sealtering Chamber (GPSC) at Nuclear Science Centre (NSC), New Delhi. The films were irradiated at varying fluences. The current was maintained at 2 pnA.

TABLE I
Details of Latices Used

Natural Rubber (NR) Latex	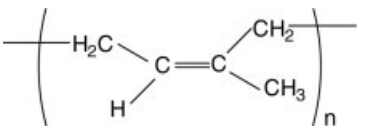
Supplied by	Gaico Rubbers Ltd., Kuravilangadu, Kottayam
Dry rubber content (DRC) (%)	60
Total solid content (TSC) (%)	61.25
Carboxylated Styrene Butadiene Rubber (XSBR) Latex (PLX-802)	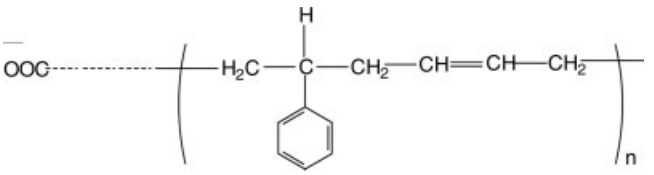
Supplied by	Apar Industries Ltd., Bombay, India
Dry rubber content (DRC) (%)	47
Total solid content (TSC) (%)	50.66
Styrene content (%)	52

Scanning electron microscopic analysis

Filler dispersion of the samples was analyzed from scanning electron micrographs of cryogenically fractured surfaces using Scanning Electron Microscope, JEOL JSM-840A.

X-ray photoelectron spectroscopy

The change in surface compositions on irradiation was determined quantitatively by X-ray photoelectron spectroscopy using SSX 100/206 Photoelectron Spectrometer from Surface Science Instruments (USA) equipped with a monochromatized microfocus Al X-ray source powered at 20 mA and 10 kV.

RESULTS AND DISCUSSION

Thermogravimetric analysis

TGA measures the change in weight of the material when it is heated in the presence of inert atmosphere or in the presence of air/oxygen. When a rubber compound is heated at lower temperature, the volatile components will get evaporated. At 100°C, water present in the rubber will get evaporated. When the heating continues, the polymer part will get degrade and converted into gaseous products, a corresponding loss in weight is reflected in the curve. Further heating will remove all organic matter, giving the weight of inorganic fillers in the compound.

Figure 1 is the TGA curves of microcomposites of NR latex films. The thermal stability of filled NR samples is lower than unfilled system. This can be explained to the aggregation of filler due to filler–filler interaction than polymer–filler interaction. During latex stage mixing, the mechanical stress applied is not sufficient to reduce the molecular weight of rubber particles to create active centers for interaction with filler. Therefore, filler aggregates can be formed in these systems. Further, it is clear from the SEM pictures presented in Figure 2. The white portion observed is the aggregates of filler particles. The nonhomogeneous distribution of filler particles decreases the thermal stability of NR. Filled samples show more residue than unfilled sample because

TABLE II
Characteristics of Fillers Used

Composition of Clay	
SiO_2 (%)	45
Al_2O_3 (%)	38
Fe_2O_3 (max.) (%)	0.5
TiO_2 (%)	0.55
CaO (max.) (%)	0.06
MgO (max.) (%)	0.07
Na_2O (max.) (%)	0.25
K_2O (max.) (%)	0.1
Loss on ignition (%)	14.5
Composition of silica	
SiO_2 (dry material) (%)	83–90
Al_2O_3 (%)	< 0.3
Na_2O (%)	0.6–2.5
Fe_2O_3 (%)	<0.04
SO_3 (%)	0.5–2.5
Drying loss (%)	8–12

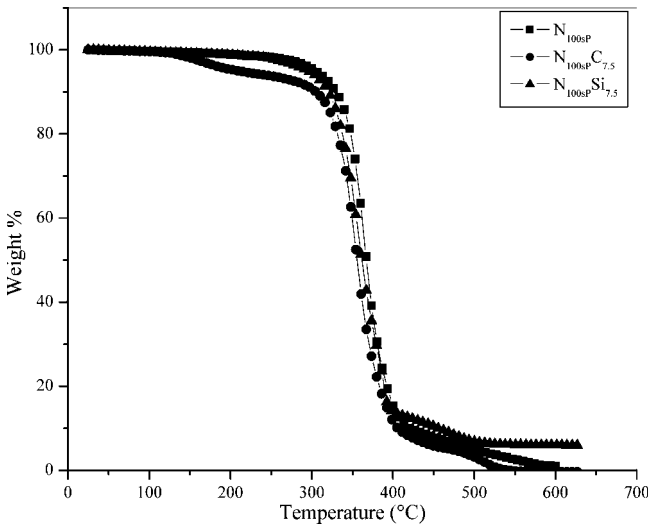

Figure 1 TGA curves of microcomposites of NR.

of the presence of inorganic fillers, which is more thermally stable. DTG curves of filled NR shows two-stage decomposition (Fig. 3). The first stage degradation is due to the deterioration of polymer chain into simple products. The second stage decomposition is the volatilization of the products formed in the first step. The decomposition temperature needed for varying weight percent of degradation is presented in Table III. It is found that the decomposition temperature is lower for micro-filled samples. The T_{max}, i.e., the temperature at maximum decomposition of filled NR also shows reduced values (Table IV). A significant delay of the thermo-degradation of XSBR matrix is observed upon the addition of microfillers (Fig. 4). This is explained to the more uniform distribution of fillers owing to the polarity of XSBR. As a result, the polymer/filler network increases leading to higher thermal stability of XSBR microcomposites. The distribution of fillers in XSBR latex is further clear from the SEM shown in Figure 5. Since XSBR is polar, the polar fillers could be nicely dispersed in the XSBR matrix. Figure 6 is the DTG curves of microfillers such as clay and silica filled XSBR latex. The filled rubber samples show three-stage decomposition corresponding to the degradation of styrene and butadiene part of polymer chain. The last degradation step may be due to the decomposition of simple products formed in the first two steps. Table III shows the degradation temperature at different percentage of weight losses for XSBR. It is found that the thermal stabilization is higher in XSBR microcomposites. Similarly, the maximum decomposition temperature of XSBR increased upon the addition of microfillers (Table IV). This can be attributable in terms of the polymer/filler interaction due to the polarity of XSBR latex.

Figure 7 is the TGA curves of microcomposites of 70/30 NR/XSBR latex blends. Filled polymer blends exhibit higher thermal stability than unfilled system. However, at intermediate position, filled and unfilled samples show similar rate of deterioration. In filled blend system, the decomposition mechanism is rather complex because of the unequal distribution of fillers into both phases. These blend systems are immiscible because of the difference in polarity of individual components. The higher thermal stability of filled blend system revealed that the major portion of the filler migrates to the XSBR phase. It is very clear from the degradation temperatures given in Table III. At different percentage of degradation the temperature is higher for filled samples. The temperature for maximum degradation and the final residue are higher in filled blend.

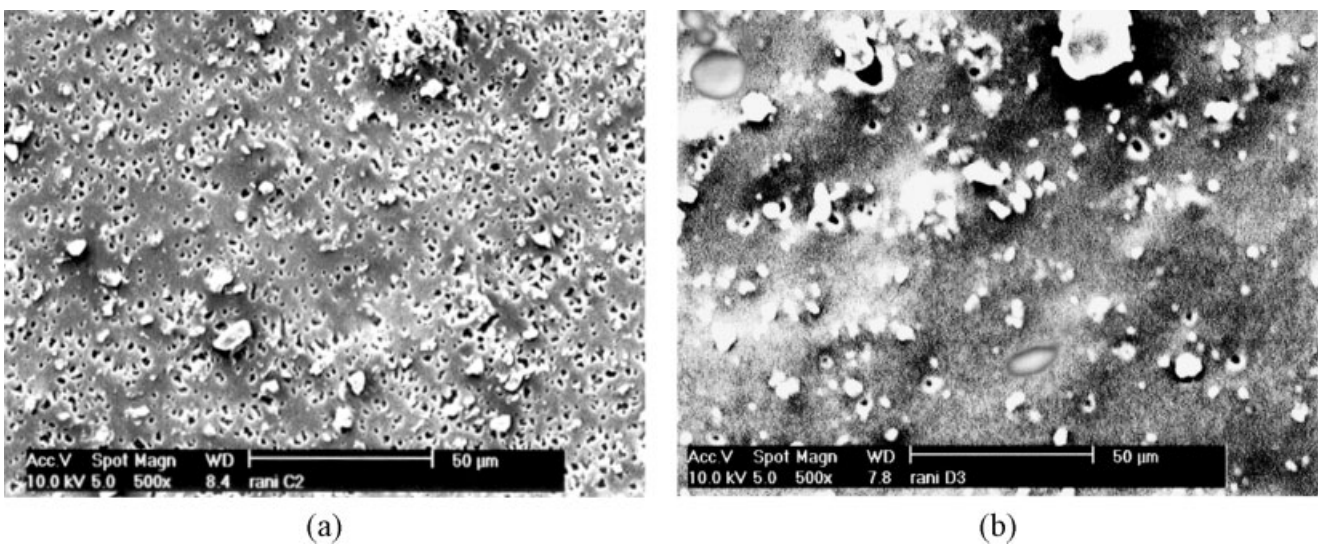

Figure 2 SEM of microcomposites of NR (a) clay and (b) Silica.

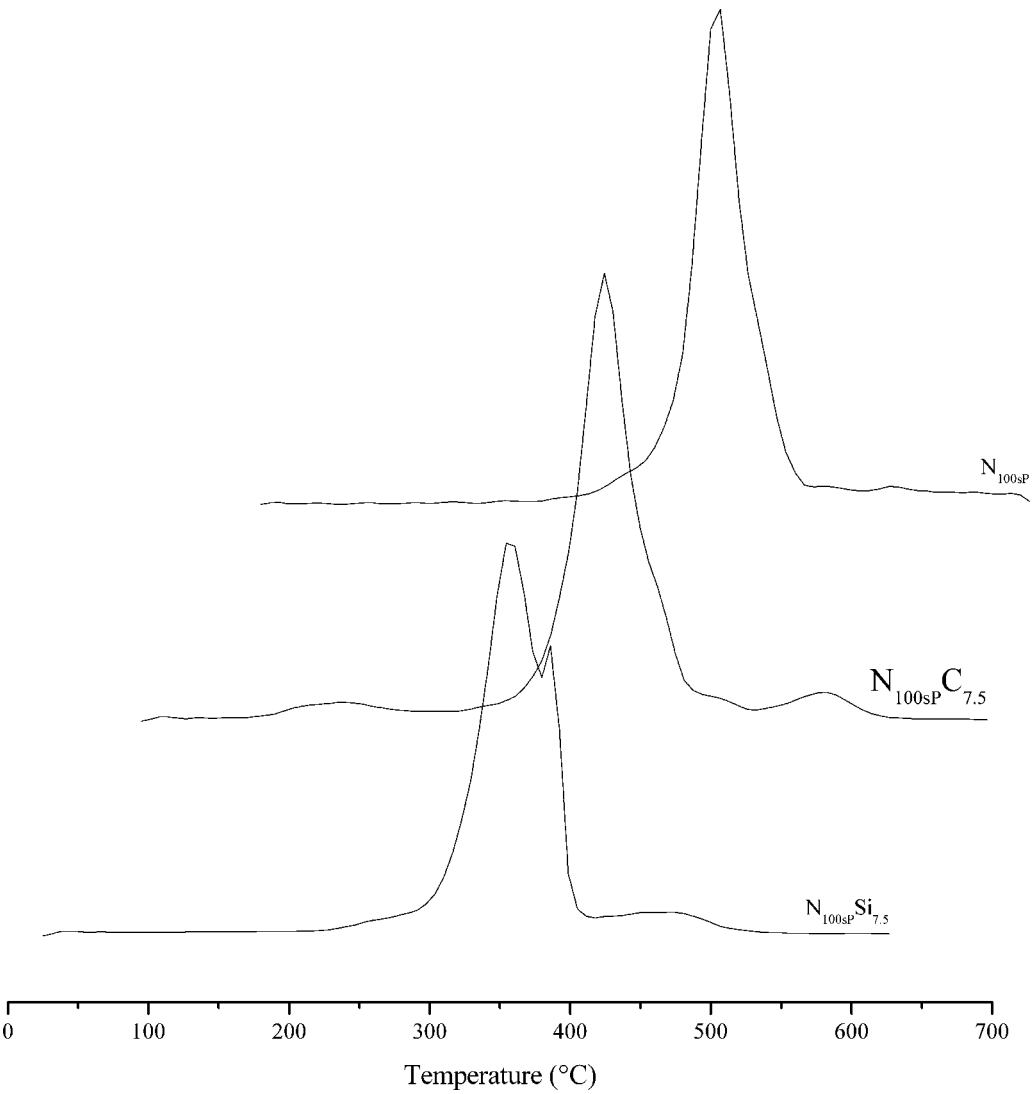

Figure 3 DTG curves of microcomposites of NR latex film.

Activation energy for degradation of microcomposites of latices

The activation energy values for degradation can give information about the thermal stability of the system. The activation energy for the degradation of microcomposites of NR, XSBR, and 70/30 NR/XSBR is determined by applying Coats-Redfern[27] equation. It is an integral method and the following equation is

TABLE III
Degradation Temperature at Different Weight Loss Levels of Micro-filled NR, XSBR, and 70/30 NR/XSBR Latices

	Degradation temperature (°C)				
Sample	$T_{10\%}$	$T_{30\%}$	$T_{50\%}$	$T_{70\%}$	$T_{90\%}$
N_{100sP}	334	355	368	384	431
$N_{100sP}C_{7.5}$	291	341	354	370	410
$N_{100sP}Si_{7.5}$	319	347	362	379	448
N_{0sP}	333	355	368	380	399
$N_{0sP}C_{7.5}$	368	380	389	420	469
$N_{0sP}Si_{7.5}$	358	375	391	422	491
N_{70sP}	343	365	381	393	449
$N_{70sP}C_{7.5}$	358	375	382	396	441
$N_{70sP}Si_{7.5}$	372	374	383	412	448

TABLE IV
Temperature at Maximum Decomposition and Residue level at 600°C of Micro-filled NR, XSBR, and 70/30 NR/XSBR Latices

Sample	T_{max} (°C)	Residue (%)
N_{100sP}	364	2.34
$N_{100sP}C_{7.5}$	360	2.54
$N_{100sP}Si_{7.5}$	359	6.00
N_{0sP}	365	1.14
$N_{0sP}C_{7.5}$	390	1.20
$N_{0sP}Si_{7.5}$	395	1.26
N_{70sP}	380	0.54
$N_{70sP}C_{7.5}$	381	0.90
$N_{70sP}Si_{7.5}$	391	1.26

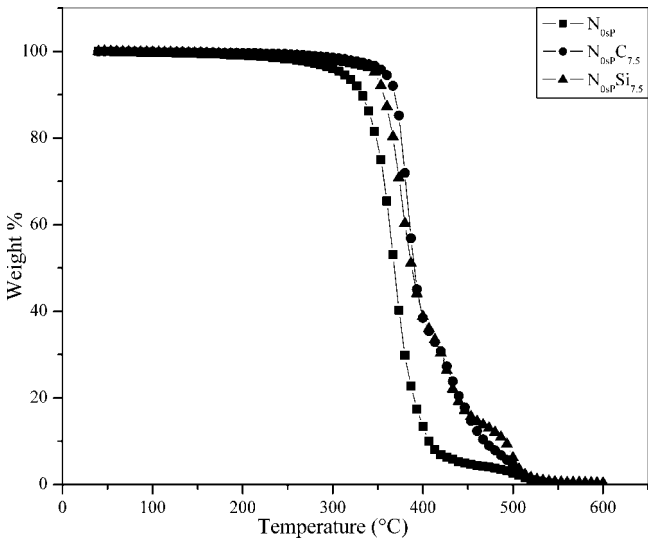

Figure 4 TGA curves of microcomposites of XSBR.

used for a first order reaction,

$$\log\left[-\log(1-\alpha)/T^2\right] = \log\left[AR/(\beta E)\left(1-2RT/E\right)\right] - E/(2.303RT) \quad (1)$$

where α is the fractional mass loss at time t, T is the absolute temperature, A is the pre-exponential factor, R is the universal gas constant, β is the heating rate, and E is the activation energy. A plot of log[−log $(1-\alpha)/T^2$] versus $1/T$ gives a straight line with the slope equal to $-E/2.303R$ and the y-intercept is log[AR/(βE) $(1-2RT/E)$].

Coats-Redfern plots of NR, XSBR, and 70/30 NR/XSBR at the main stage decomposition are shown in Figures 8–11. The activation energy is computed from Coats-Redfern plot. The activation energy values obtained for various microcomposites of samples are presented in Table V. It is found that the activation energy required for the thermal degradation of microcomposites of XSBR and 70/30 NR/XSBR samples is higher than pristine polymer. However, for filled NR, the values are lower than gum sample due to the poor interaction of filler with the polymer. The higher thermal stability of microcomposites of XSBR and 70/30 NR/XSBR indicate better dispersion of filler in the rubber matrix. The enhanced thermal stability of XSBR and 70/30 NR/XSBR is owing to the reinforcement caused by the incorporation of particulate fillers. The reinforcement of fillers can also be predicted by using Kraus equation.[28] The equation is

$$V_{ro}/V_{rf} = 1 - m(f/1-f) \quad (2)$$

where V_{rf} is the volume fraction of rubber in the solvent-swollen filled sample and is given by

$$V_{rf} = \frac{(d-fw)/\rho_P}{d-fw/\rho_P + A_S/\rho_S} \quad (3)$$

where d is the deswollen weight, f is the volume fraction of the filler, w is the initial weight of the sample, ρ_P is the density of the polymer, ρ_S is the density of the solvent, and As is the amount of solvent absorbed. V_{ro} is

$$V_{ro} = \frac{d/\rho_P}{d/\rho_P + A_S/\rho_S} \quad (4)$$

A plot of V_{ro}/V_{rf} as a function of $(f/1-f)$ should give a straight line with slope m. The value of m is a direct measure of the reinforcing ability of the filler used. According to this theory, reinforcing fillers have negative slope, indicating better polymer–filler

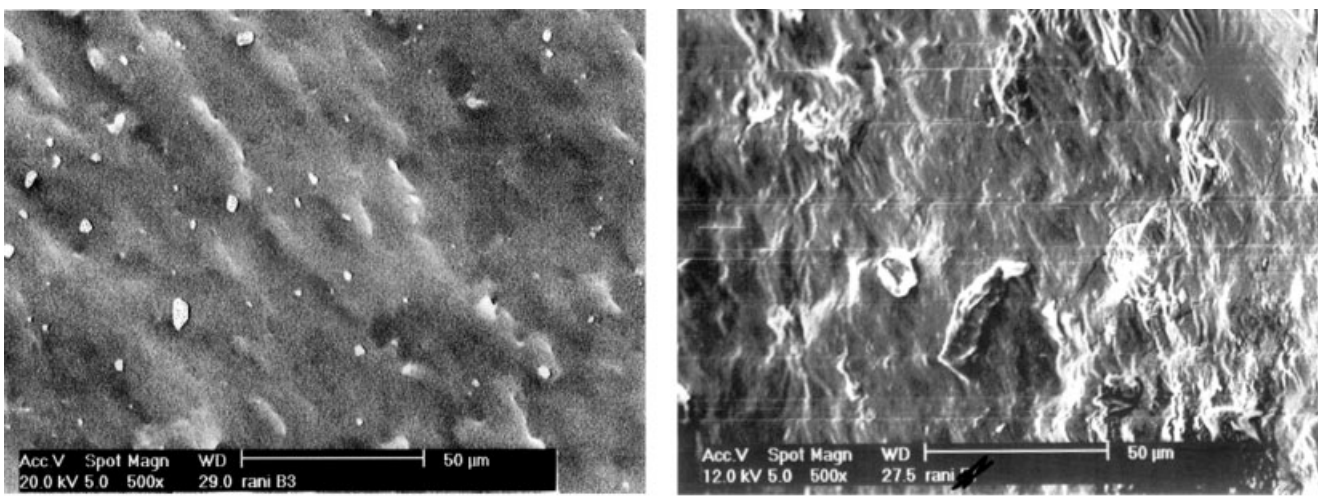

Figure 5 SEM of microcomposites of XSBR (a) clay and (b) silica.

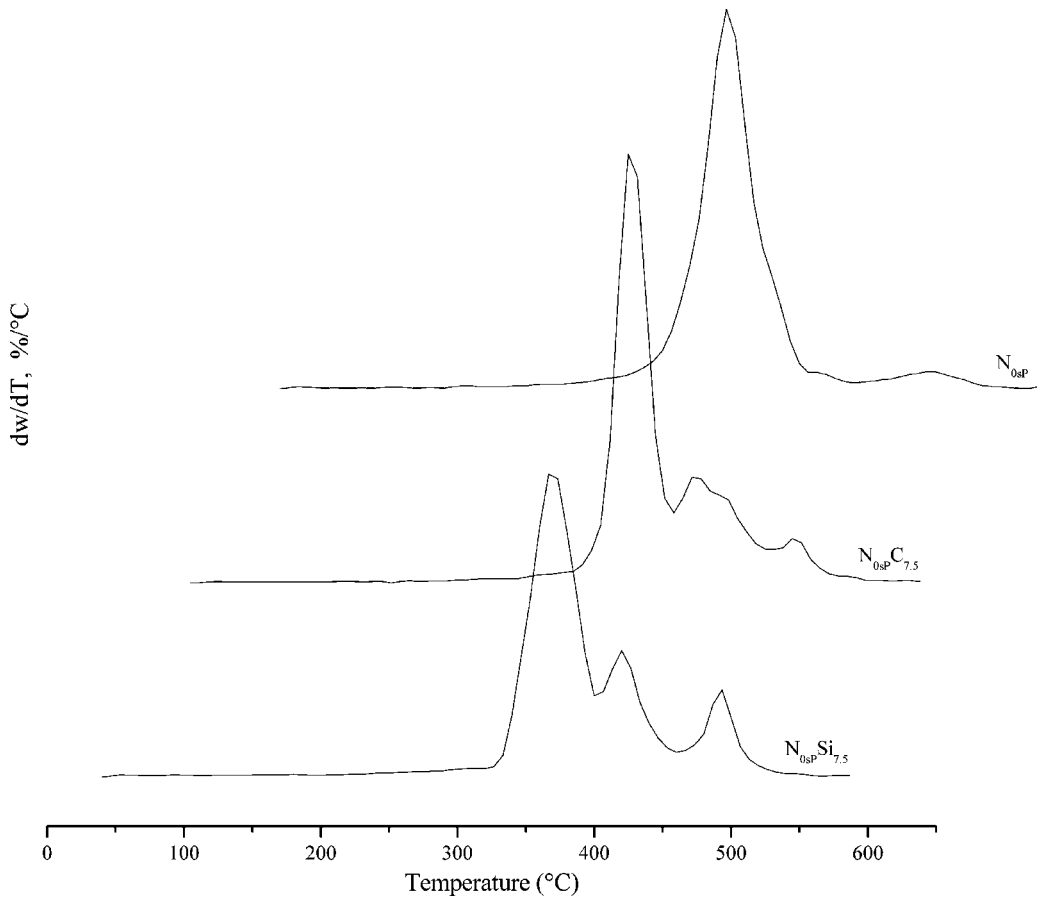

Figure 6 DTG curves of microcomposites of XSBR.

interaction. The value of *m* reflects the polymer–filler interaction clearly.

Kraus plots of microcomposites of NR, XSBR and 70/30 NR/XSBR are given in Figures 12 and 13. It can be seen that clay filled XSBR show negative m value, which denote the reinforcement of filler in the rubber matrix. For clay filled NR and 70/30 NR/XSBR, the Kraus plots deviate different degrees upward direction, give positive *m* value, indicating poor rubber–filler interaction. Silica filled XSBR and 70/30 NR/XSBR gives negative *m* values. The superior reinforcing action of fillers in XSBR matrix is due to their high interaction with the polar XSBR polymer surface. The data obtained from Kraus plots shows the high extent of polymer/filler interaction in the case of XSBR system. The high polymer/filler interaction is responsible for the superior thermal stability.

Ageing resistance

Knowledge on ageing characteristics of latex goods is relevant for determining their service life. The crosslinked rubber chain may undergo scission as well as crosslinking reactions during service life at elevated temperatures. During ageing of rubber vulcanizates, the breaking down of polysulphidic crosslinks occurs. For rubber vulcanizates excellent tensile strength, rebound resilience, and flex fatigue properties are obtained with polysulphidic crosslinks,

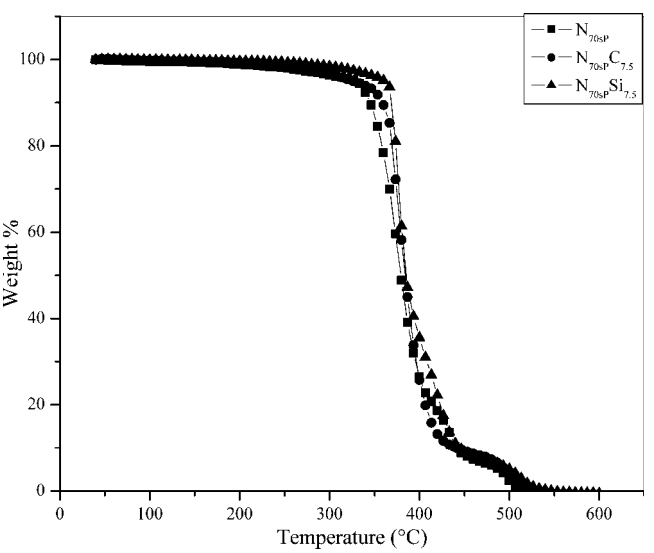

Figure 7 TGA curves of microcomposites of 70/30 NR/XSBR.

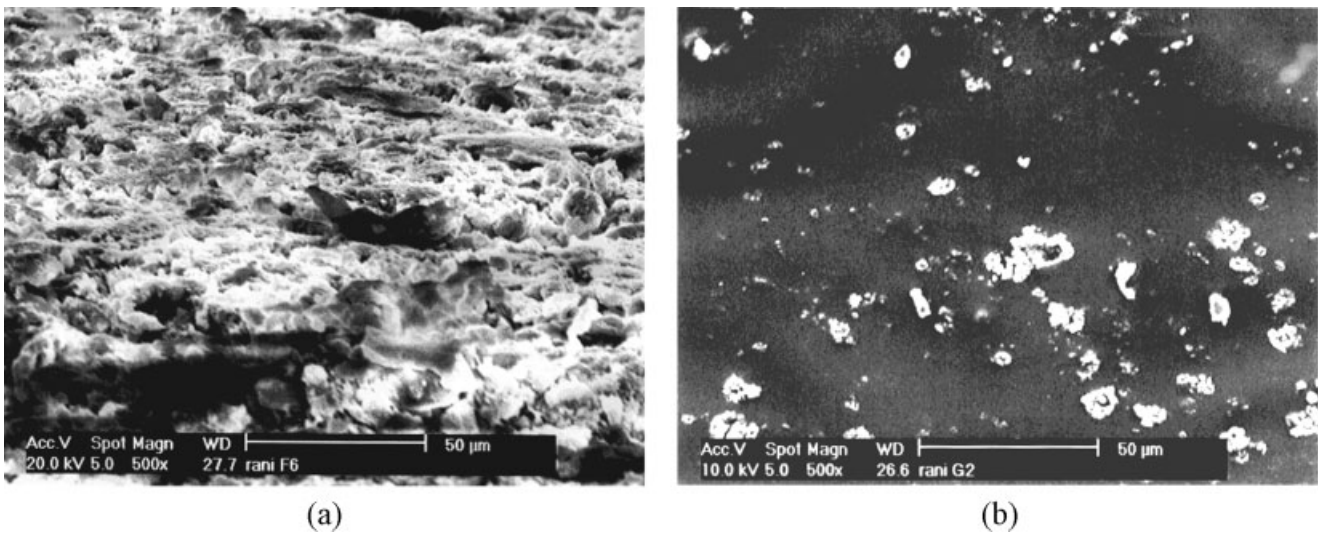

Figure 8 SEM of microcomposites of 70/30 NR/XSBR (a) clay and (b) silica.

whereas resistance to heat ageing and compression set are best with shorter crosslinks.[29] Therefore, an understanding of the mechanical properties of aged samples is important for the end product applications. The addition of fillers to polymer can improve the ageing resistance depending upon the polymer and the filler used.

Thermal ageing

Figure 14 is the relative tensile strength versus filler loading of NR. The relative tensile strength is used as an indicator for determining the resistance to thermal ageing. The higher is the relative tensile strength the higher is the thermal resistance. It is observed that the relative tensile strength increases as a function of increase in filler concentration. The increase in value indicates the ageing resistance of filled NR. This can be explained in terms of the barrier effect of filler present in the polymer surface, which will resist the degradation. A plot of relative tensile strength as a function of filler concentration of XSBR is given in Figure 15. As the filler concentration increases, the relative tensile strength of XSBR also increases. Silica filled XSBR exhibits significant increase. It is due to the polar–polar interaction between the polymer and the filler. Figure 16 is the relative tensile strength versus filler concentration of 70/30 NR/XSBR blends. It can be seen that upon the addition of filler the relative tensile strength value increases. However, for clay filled blend, it decreases at higher concentration because of the agglomeration of filler particles. The modulus at 300% elongation and strain at break (%) of aged micro-filled NR,

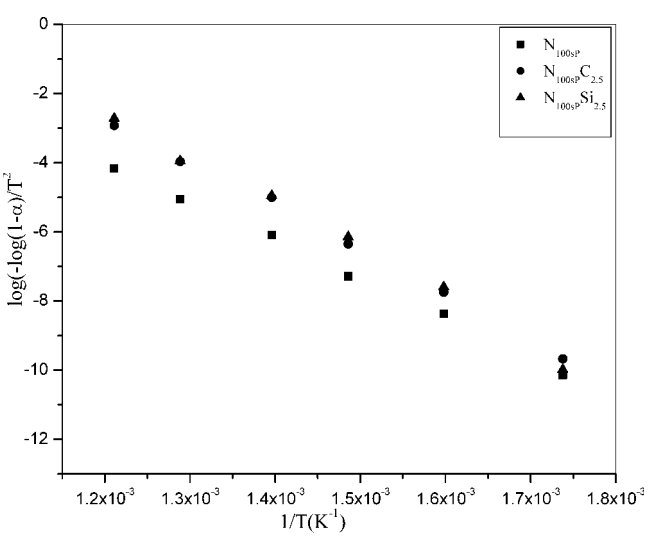

Figure 9 Coats-Redfern plots of microcomposites of NR.

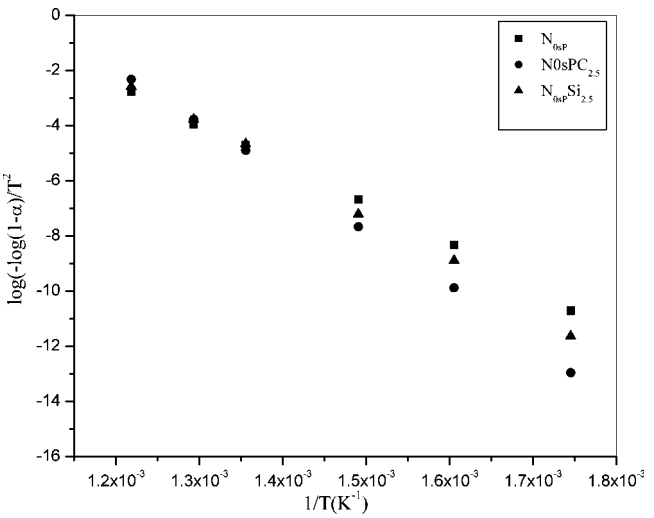

Figure 10 Coats-Redfern plots of microcomposites of XSBR.

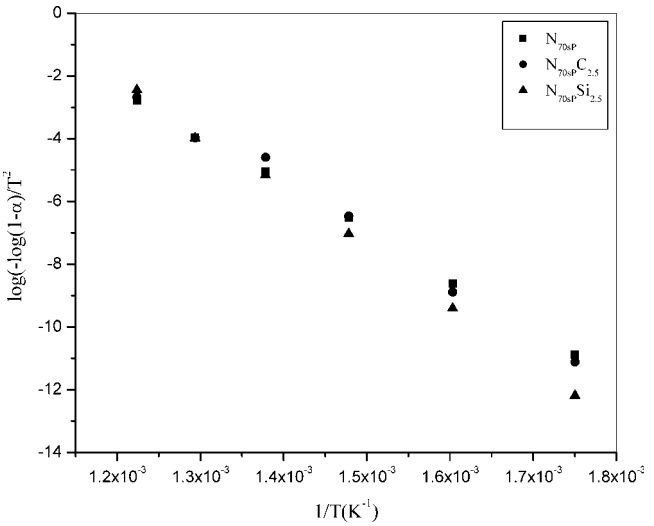

Figure 11 Coats-Redfern plots of microcomposites of 70/30 NR/XSBR.

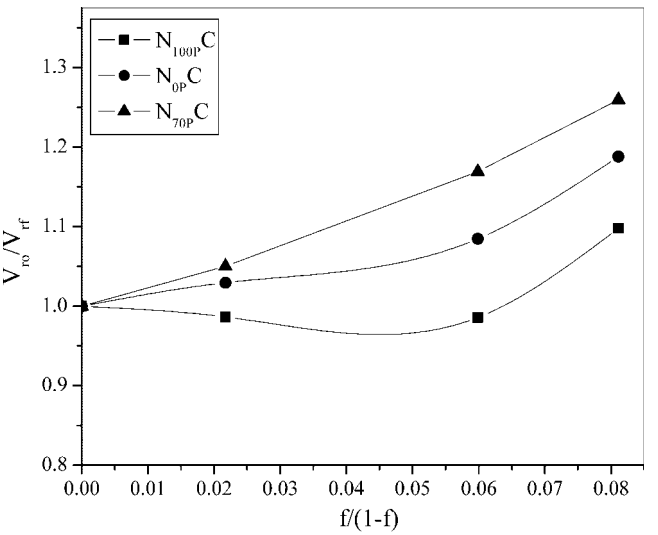

Figure 12 Kraus plot of clay filled NR, XSBR, and 70/30 NR/XSBR latex films.

XSBR, and 70/30 NR/XSBR latices are presented in Table VI. It can be seen that the modulus of aged filled and unfilled XSBR increases. This is explained to the formation of crosslinks on heating. It is found that before aging the clay filled system shows decrease in modulus due to the adsorption of curatives on the filler surface. As a result the crosslink density decreases. However, after aging the clay filled system exhibits higher modulus. This explained to the crosslinking of unreacted curatives upon heating. Strain at break (%) of all the samples is found to be decreasing upon ageing.

Irradiation ageing

XPS is an efficient tool for measuring the surface microcharacteristics, chemical states and compositions of ion bombarded polymeric materials. The binding energies of C_{1s}, O_{1s}, and Si_{2p} of silica filled unirradiated and irradiated NR, XSBR, and 70/30 NR/XSBR are given in Table VII. The binding energies of unirradiated systems for C_{1s}, O_{1s}, and Si_{2p} are 285.8, 533.1, and 102.9 respectively, for NR. The binding energies of C_{1s}, O_{1s}, and Si_{2p} show almost same values for all system before and after irradiation. The unchanged binding energy values indicate the redistribution of elements within the system upon ion-beam irradiation.

The peak area of C_{1s}, O_{1s}, and Si_{2p} are given in Table VIII. For NR at lower fluence the peak area of C_{1s} increased and then decreased at higher fluence, indicating chain depletion. The peak area of O_{1s} decreases with increase in fluence. The area of Si_{2p} increases with ion fluence and can be explained in terms of ion implantation during irradiation. In the case of XSBR the area of the peak C_{1s} and O_{1s} shows

TABLE V
Activation Energy of Degradation of Micro-filled NR, XSBR, and 70/30 NR/XSBR Latices

Sample	Activation energy (kJ/mol)
N_{100sP}	483
$N_{100sP}C_{7.5}$	409
$N_{100sP}Si_{7.5}$	443
N_{0sP}	493
$N_{0sP}C_{7.5}$	603
$N_{0sP}Si_{7.5}$	505
N_{70sP}	440
$N_{70sP}C_{7.5}$	472
$N_{70sP}Si_{7.5}$	505

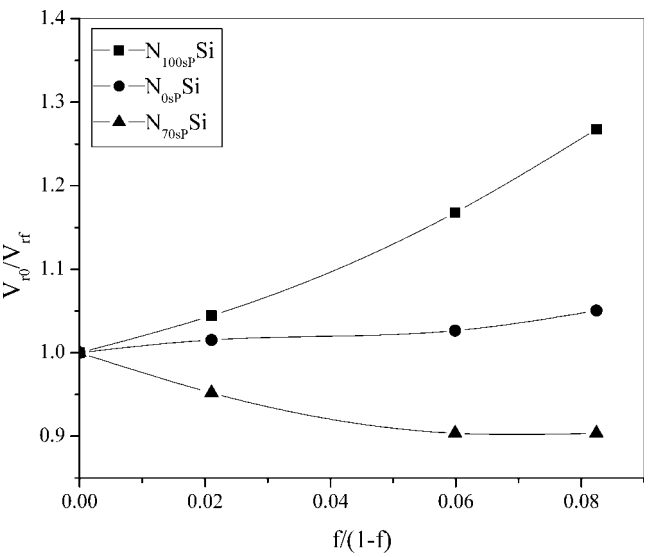

Figure 13 Kraus plots of silica filled NR, XSBR, and 70/30 NR/XSBR latex films.

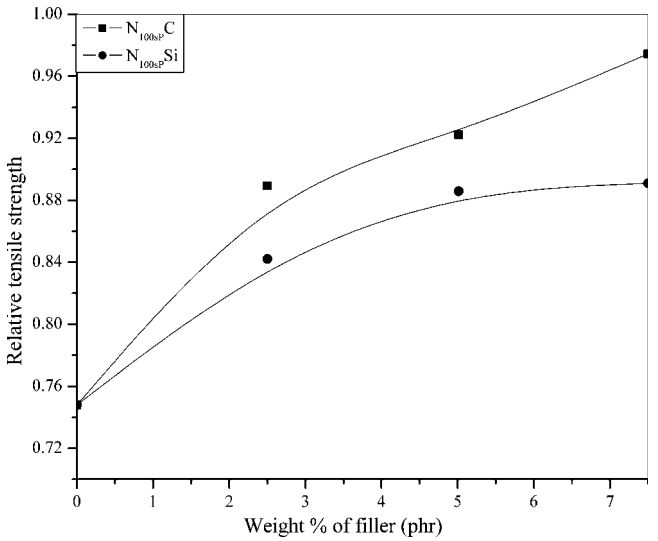

Figure 14 Tensile strength versus filler loading graph of unaged and aged microcomposites of NR.

steep rise with ion fluence. The Si_{2p} peak area of XSBR increases constantly with fluence similar to that of NR.

The 70/30 NR/XSBR shows decrease in peak area of C_{1s} and O_{1s} compared to unirradiated. The minimum peak area can be observed at lower fluence. The change in peak area of Si_{2p} is quite different from the virgin polymers. The unirradiated system itself shows lower Si_{2p} peak area when compared to unirradiated NR and XSBR. This is due to the uneven distribution of silica filler in the two phases. In this case XSBR is dispersed in the continuous NR matrix. At lower fluence the Si_{2p} peak area increases while at higher fluence it decreases.

A clear picture of the solvent resistance of the samples can be obtained from the swell ratio. The

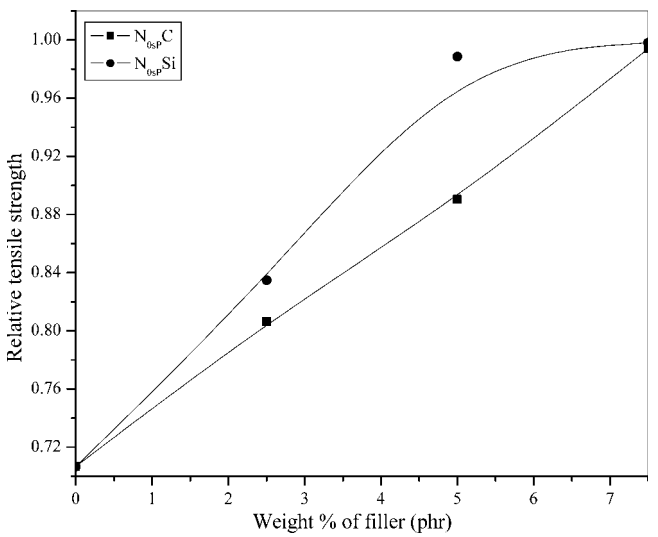

Figure 15 Tensile strength versus filler loading graph of unaged and aged microcomposites of XSBR.

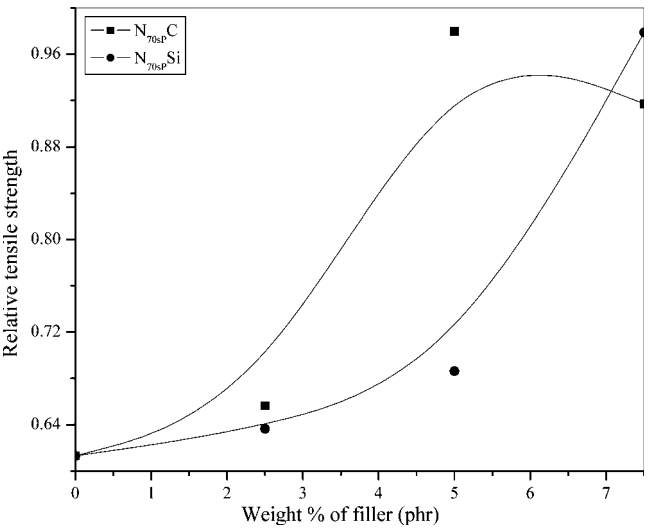

Figure 16 Tensile strength versus filler loading graph of unaged and aged microcomposites of 70/30 NR/XSBR.

swell ratio values are higher for NR, indicating that it is less resistant to solvent. The swell ratio values are lower for XSBR. Ion beam irradiated filled XSBR are more resistant to solvents.

CONCLUSIONS

Thermal stability and ageing resistance of microcomposites of NR, XSBR latices, and their 70/30 NR/XSBR blend were investigated. It was found that the addition of microfillers improved degradation stability of XSBR and 70/30 NR/XSBR blends. The microcomposites of NR showed reduced thermal stability due to its poor interaction with filler. The activation energy required for thermal degradation was determined from Coats-Redfern plots. The values obtained were higher for filled XSBR and 70/30 NR/XSBR latex blends than for NR. The higher the activation energy the higher will be the thermal stability. The reinforcement occurred in XSBR and 70/30 NR/XSBR

TABLE VI
Modulus at 300% Elongation and Elongation at Break (%) of Unaged and Aged Micro-filled NR, XSBR, and 70/30 NR/XSBR Latices

	Modulus at 300 % elongation (MPa)		Elongation at break (%)	
Sample	Unaged	Aged	Unaged	Aged
N_{100sP}	0.57	0.52	1114	1181
$N_{100sP}C_{7.5}$	0.55	0.57	1274	1041
$N_{100sP}Si_{7.5}$	–	0.53	–	1183
N_{0sP}	1.75	1.76	458	420
$N_{0sP}C_{7.5}$	1.39	2.22	548	355
$N_{0sP}Si_{7.5}$	1.29	2.08	392	247
N_{70sP}	0.72	0.67	1189	792
$N_{70sP}C_{7.5}$	0.59	0.67	1084	770
$N_{70sP}Si_{7.5}$	0.86	0.66	869	748

TABLE VII
Binding Energy of Unirradiated and Irradiated Silica-filled NR, 70/30 NR/XSBR, and XSBR Latices

	Binding energy (eV)		
	Unirradiated	Low Fluence (ions/cm^2)	High fluence (ions/cm^2)
Silica-filled NR			
C_{1s}	285.8	285	285
O_{1s}	533.1	533.6	532.5
Si_{2p}	102.9	103.4	104.6
Silica-filled NR/XSBR			
C_{1s}	284.7	285.2	285.1
O_{1s}	532	533.6	533.4
Si_{2p}	103	103.5	103.3
Silica-filled XSBR			
C_{1s}	285.6	285.3	284.8
O_{1s}	532.8	533.7	532.2
Si_{2p}	102.8	102.5	103.1

in the presence of microfillers was further confirmed from Kraus plots. The negative slope values obtained for XSBR and XSBR-rich blend indicated the reinforcement of filler in rubber matrix. The polymer films of clay and silica filled and unfilled NR, 70/30 NR/XSBR were irradiated using Si ion. The X-ray photoelectron spectrum of silica filled latex films unirradiated and irradiated at lower and higher fluences were analyzed. The results of XPS measurements showed that the binding energies of C_{1s}, O_{1s}, and Si_{2p} remain intact on irradiation and indicated that the host elements were redistributed in latex films. Irradiated samples showed decreased swell ratio values because of the formation of crosslinks through electronic excitation on irradiation.

TABLE VIII
Peak Area of Unirradiated and Irradiated Silica-filled NR, 70/30 NR/XSBR, and XSBR Latices

	Peak area		
	Unirradiated	Low Fluence	High fluence
Silica-filled NR			
C_{1s}	5209.9	6519.7	4970.9
O_{1s}	3021.2	2255.2	1717
Si_{2p}	87.4	183.4	192
Silica-filled NR/XSBR			
C_{1s}	3582.8	2902.1	3079
O_{1s}	1242	917.8	1072.9
Si_{2p}	42.5	99.6	13.4
Silica-filled XSBR			
C_{1s}	3598.8	3124.5	7144.1
O_{1s}	1942	1210.7	2626.3
Si_{2p}	78.3	95.9	139.7

One of the authors Ms. Ranimol Stephen is thankful to IUAC, New Delhi for providing the Junior Research Fellowship and the facilities for ion-beam irradiation.

References

1. Callum, J. R. M. Comprehensive Polymer Science: The synthesis, Characterisation, Reactions and Applications of Polymers, Vol. 1: Polymer Characterisation, 1st ed.; Pergamon Press: 1989; p 903.
2. Still, R. H. In Developments in Polymer Degradation, Vol. 1; Grassie, N., Eds.; Applied Science: London, 1977; p 1.
3. Byers, J. T. Rubber World 1998, 219, 38.
4. Choi, S. S. J Appl Polym Sci 2001, 79, 1127.
5. Venter, S. A. S.; Kunita, M. H.; Matos, R.; Nery, R. C.; Radovanovic, E.; Muniz, E. C.; Girotto, E. M.; Rubira, A. F. J Appl Polym Sci 2005, 96, 2273.
6. Pattanawanidchai, S.; Saeoui, P.; Sirisinha, C. J Appl Polym Sci 2005, 96, 2218.
7. Stephen, R.; Raju, K. V. S. N.; Nair, S. V.; Varghese, S.; Oommen, Z.; Thomas, S. J Appl Polym Sci 2003, 88, 2639.
8. Stephen, R.; Thomas, S.; Joseph, K. J Appl Polym Sci, to appear.
9. Koshy, A. T.; Kuriakose, B.; Thomas, S. Polym Degrad Stab 1992, 36, 137.
10. Varghese, S.; Kuriakose, B.; Thomas, S. Polym Degrad Stab 1994, 44, 55.
11. Joseph, K.; Thomas, S.; Pavithran, C. Compos Sci Technol 1995, 53, 99.
12. Varghese, H.; Bhagawan, S. S.; Thomas, S. J Therm Anal Calor 2001, 63, 749.
13. Varkey, J. T.; Augustine, S.; Thomas, S. Polym Plast Technol Eng 2000, 39, 415.
14. Li, S.-D.; Cheung, M. K.; Zhong, J.-P.; Yu, H.-P. J Appl Polym Sci 2001, 82, 2590.
15. Lee, E. H.; Lee, Y.; Oliver, W. C.; Mansur, L. K. J Mater Res 1993, 8, 377.
16. Lee, E. H. Nucl Instrum Methods Phys Res Sect B 1999, 15, 129.
17. Ruck, D. M.; Schulz, J.; Deusch, N. Nucl Instrum Methods Phys Res Sect B 1997, 131, 149.
18. Rizzatti, M. R.; Araujo, M. A.; Livi, R. P. Nucl Instrum Methods Phys Res Sect B 1994, 91, 450.
19. Lee, E. H. Polyimide: Fundamental Aspects and Technological Applications; Marcel Dekker: New York, 1995.
20. Rizzatti, M. R.; Araujo, M. A.; Livi, R. P. Surf Coat Technol 1995, B70, 197.
21. Singh, L.; Singh, R. Nucl Instrum Methods Phys Res Sect B 2004, 225, 478.
22. Takahashi, S.; Yoshida, M.; Asano, M.; Notomi, M.; Nakagawa, T. Nucl Instrum Methods Phys Res Sect B 2004, 217, 435.
23. Calcagno, L.; Compagnini, G.; Foti, G. Nucl Instrum Methods Phys Res Sect B 1992, 65, 413.
24. Abel, F.; Quillet, V.; Schott, M. Nucl Instrum Methods Phys Res Sect B 1995, 105, 86.
25. Zhu, Z.; Sun, Y.; Liu, C.; Liu, J.; Jin Y. Nucl Instrum Methods Phys Res Sect B 2002, 193, 271.
26. Rangel, E. C.; Cruz, N. C.; Lepienski, C. M. Nucl Instrum Methods Phys Res Sect B 2002, 191, 704.
27. Coats, W.; Redfern, J. P. Nature 1964, 201, 68.
28. Kraus, G. Rubber Chem Technol 1978, 67, 1.
29. Haghighat, M.; Zadhoush, A.; Khorasani, S. N. J Appl Polym Sci 2005, 96, 2203.